

Supporting Information

Engineering 3D Well-Interconnected Na₄MnV(PO₄)₃ Facilitates Ultrafast and Ultrastable Sodium Storage

Wei Zhang,[†] Zhian Zhang,^{*,†} Huangxu Li,[†] Dapeng Wang,[†] Taosheng Wang,[†] Xuewen Sun,[†] Jingqiang Zheng,[†] Yanqing Lai^{*,†}

[†] School of Metallurgy and Environment, Central South University, Changsha 410083, P. R. China

Corresponding Authors

* E-mail: zhangzhian@csu.edu.cn (Z.Z.).

* E-mail: laiyanqingcsu@163.com (Y.L.).

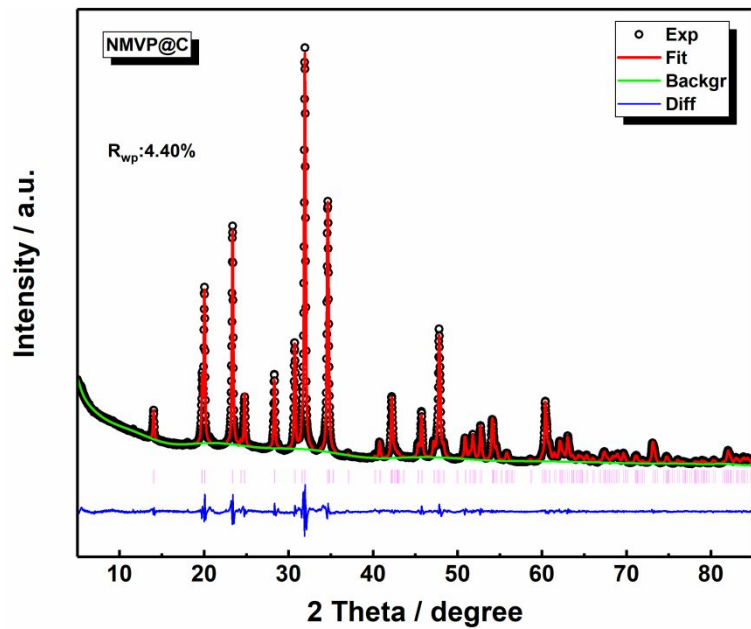


Figure S1. Rietveld refinement pattern of XRD results for NMVP@C.

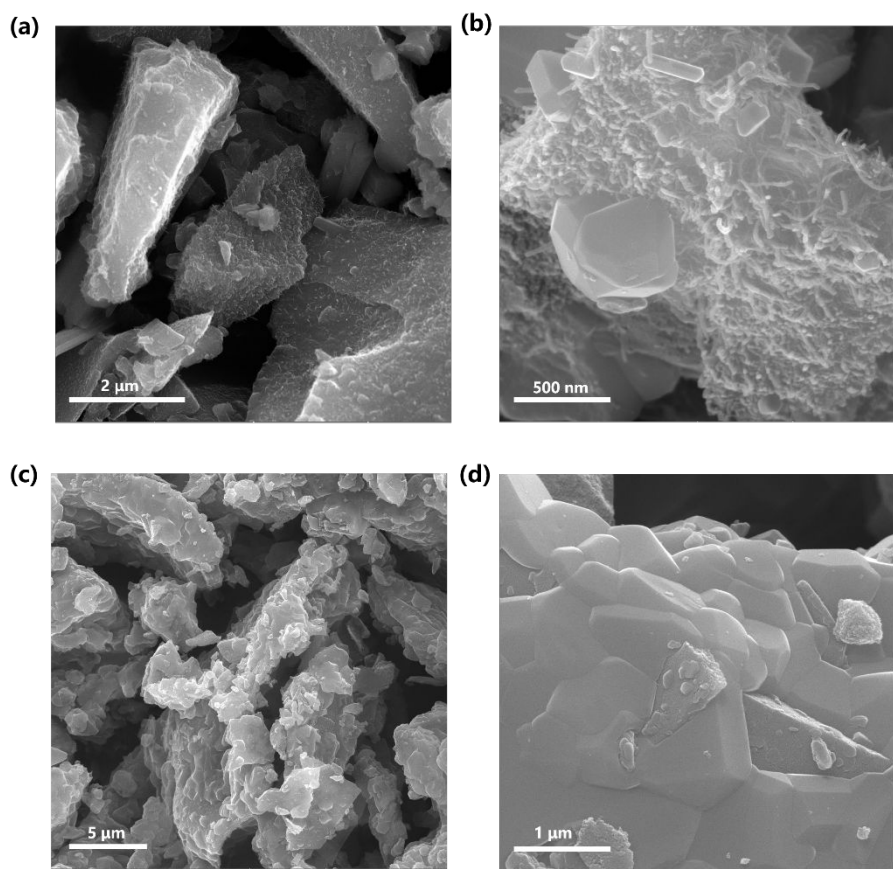


Figure S2. SEM images of (a and b) NMVP@C@CNTs and (c and d) NMVP@C samples.

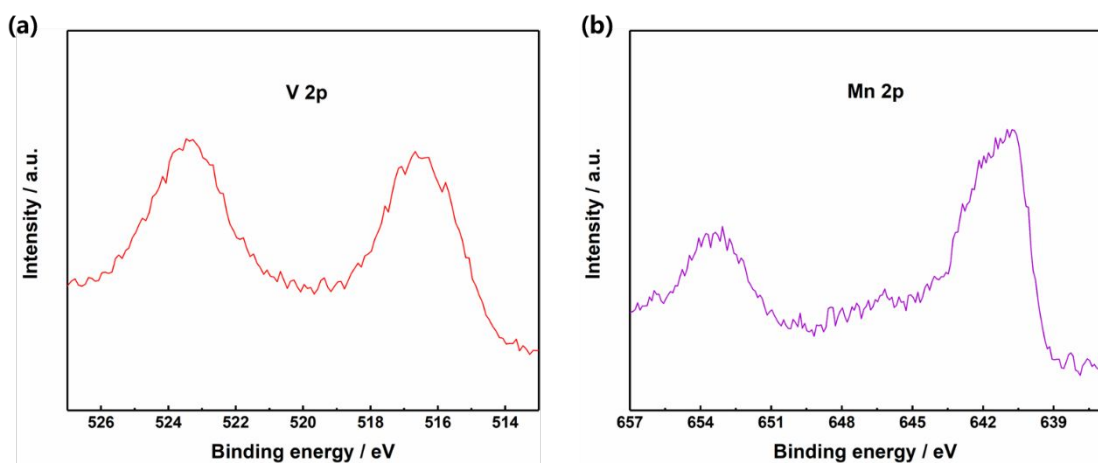


Figure S3. Core-level XPS spectra of a) V 2p, and b) Mn 2p for NMVP@C sample.

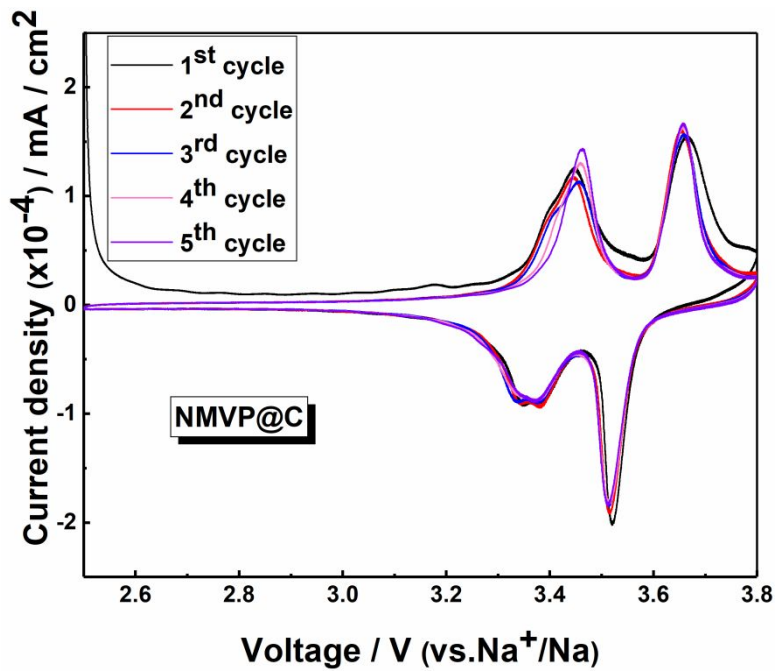


Figure S4. Cyclic voltammetry (CV) curves for the first 5 cycles of NMVP@C electrode at a scan rate of 0.1 mV s^{-1} (vs. Na $^+$ / Na).

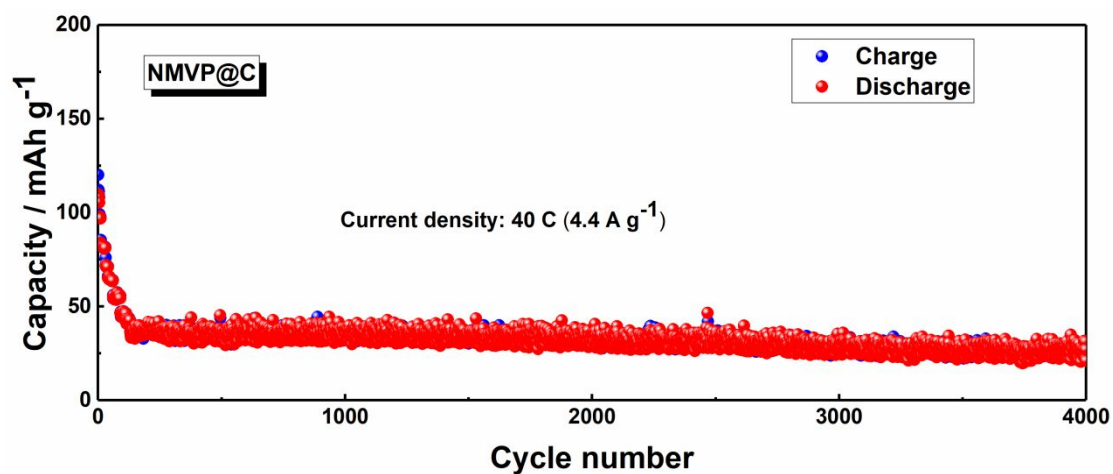


Figure S5. Cycling stability of the NMVP@C electrode for 4000 cycles at ultrahigh-rate of 40 C.

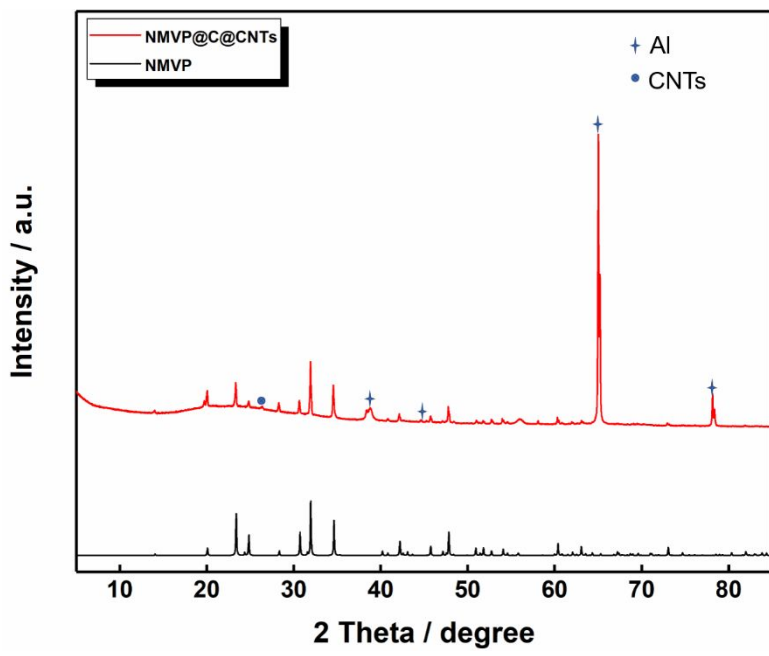


Figure S6. XRD pattern of the NMVP@C@CNTs after 4000 cycles at 40 C.

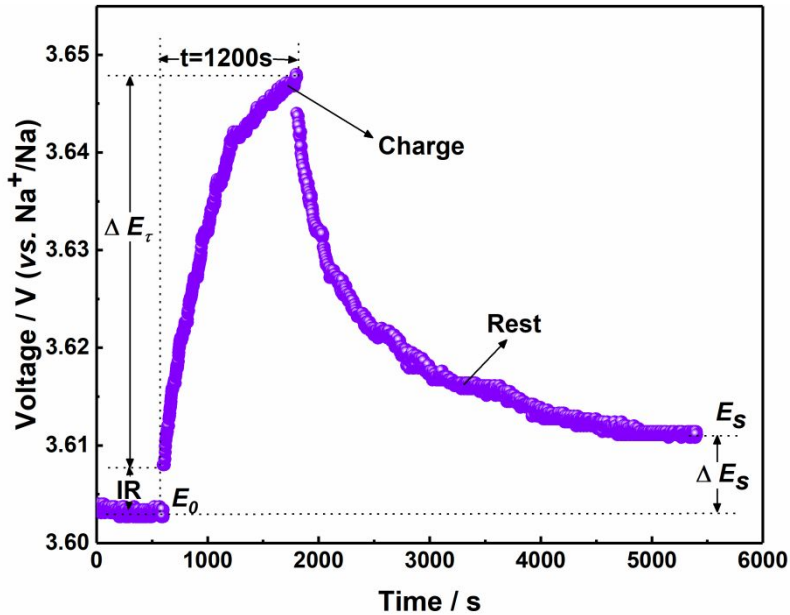


Figure S7. Detailed schematic diagram of a single-step GITT experiment at $\sim 3.60\text{V}$ for NMVP@C@CNTs composite. (Current density: 0.075 C , 8.25 mA g^{-1}).

The charging time was set at 1200 s (τ), followed by a rest process lasted 3600 s . For calculating the diffusion coefficient of sodium ions (D), the equation can be as follows¹:

$$D = \frac{4}{\pi\tau} \left(\frac{m_B V_m}{M_B S} \right)^2 \left(\frac{\Delta E_s}{\Delta E_\tau} \right)^2 \quad (\tau \ll L^2/D) \quad (\text{S1})$$

Where L , m_B , M_B , V_m , S represent the thickness of the loading slurry, mass, molecular weight, molar volume, surface area of the NMVP@C@CNTs cathode material.

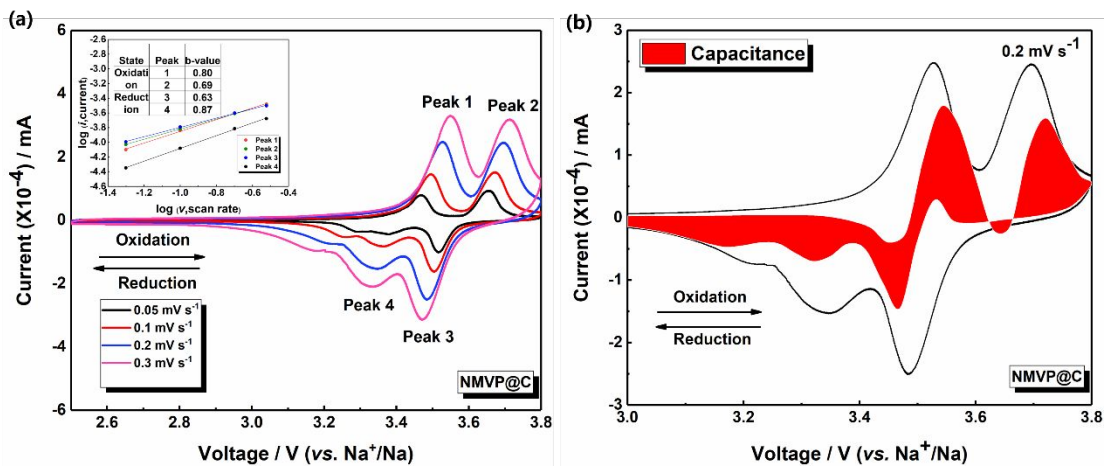


Figure S8. (a) CV curves of NMVP@C cathode at different scan rate; the inset is the log (*i*) as a function of log (*v*) at different redox states; (b) The calculated capacitance contribution (red region) for the CV curve of NMVP@C at a scan rate of 0.2 mV s⁻¹ (vs. Na⁺/Na).

The pseudocapacitive contributions to Na storage in NMVP@C@CNTs and NMVP@C nanocomposites could be further investigated by using the following equations²:

$$i_p = av^b \quad (\text{S2})$$

$$\log (i_p) = b \times \log(v) + \log a \quad (\text{S3})$$

$$i(V)/v^{1/2} = k_1 v^{1/2} + k_2 \quad (\text{S4})$$

Where *a*, *b*, *k*₁, and *k*₂ are adjustable parameters. *v*, *i* represent scan rate and current, respectively.

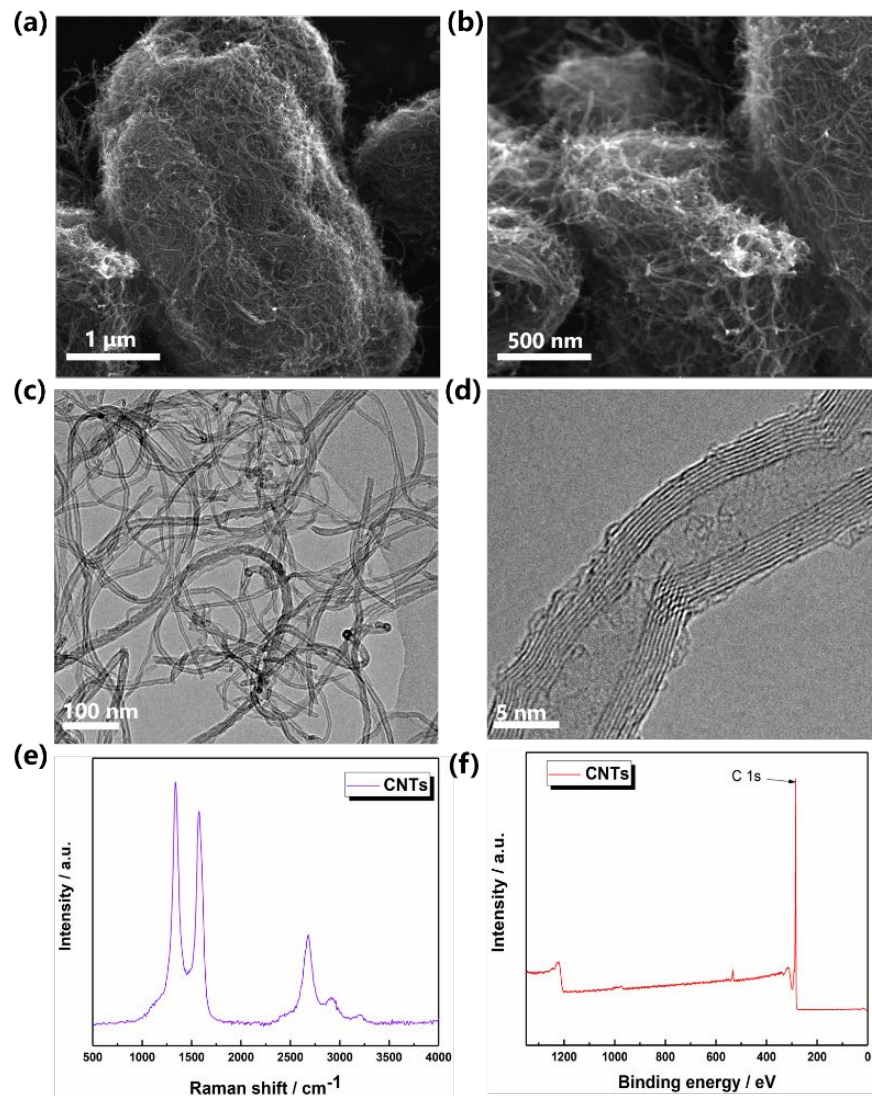


Figure S9. (a and b) SEM images, (c) TEM image, (d) HRTEM image, (e) Raman spectra and (f) XPS spectra of the CNTs.

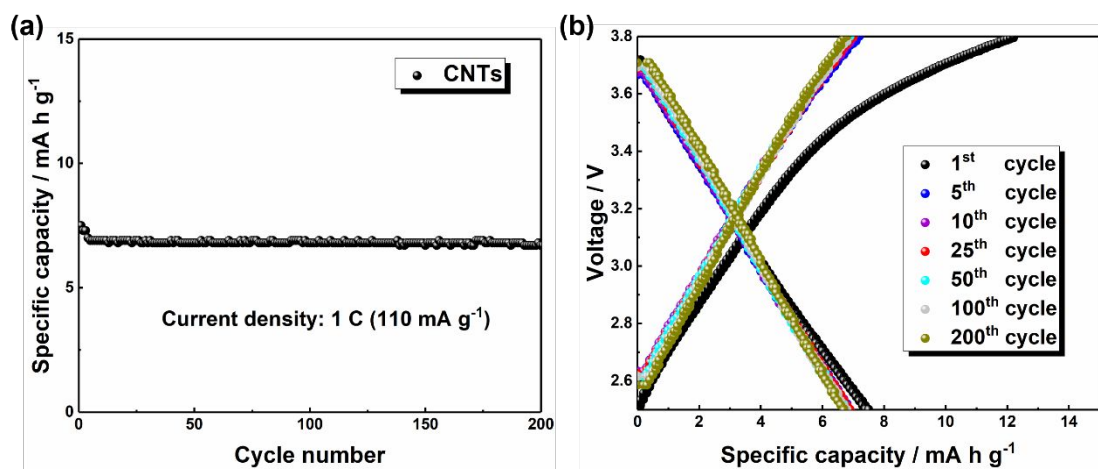


Figure S10. (a) Cycling performance and (b) corresponding charge/discharge curves in different cycles of CNTs material as cathode for sodium-ion batteries at 1 C (110 mA g^{-1}) in a voltage range of 2.5-3.8 V vs. Na^+/Na .

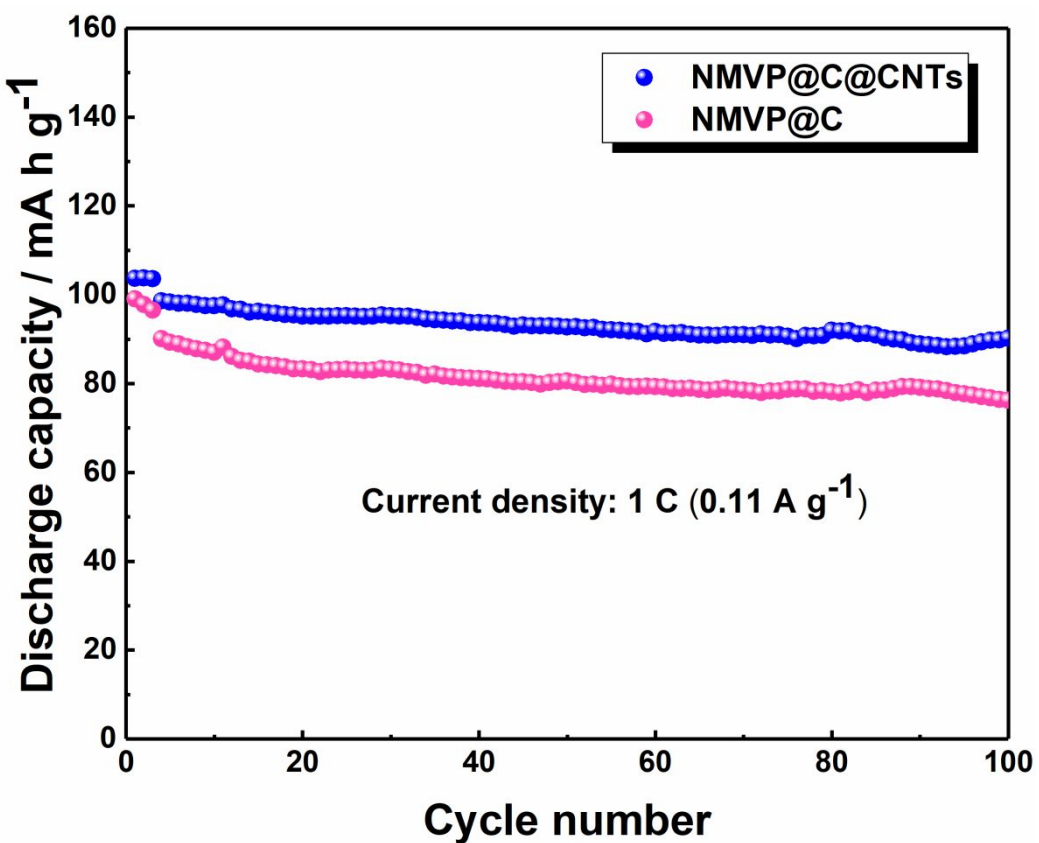


Figure S11. Cycling performance of both samples at 1 C.

Table S1. Detailed structural information of NMVP@C derived from Rietveld refinement.

Space group = R-3c	$R_{wp} = 4.40\%$	$R_p = 3.12\%$		
$a (\text{\AA}) = 8.95294$	$c (\text{\AA}) = 21.49638$	$\alpha (^\circ) = 90$		
$\beta (^\circ) = 90$	$\gamma (^\circ) = 120$	$V (\text{\AA}^3) = 1492.201$		
Atom	x	y	z	frac
Na1	0.00000	0.00000	0.00000	1.040
Na2	0.64133	0.00000	0.25000	0.971
Mn	0.00000	0.00000	0.15324	0.500
V	0.00000	0.00000	0.14280	0.500
P	0.29423	0.00000	0.25000	1.000
O1	0.02665	0.21927	0.19422	1.000
O2	0.18456	0.17371	0.08788	1.000

Table S2. Detailed structural information of NMVP@C@CNTs derived from Rietveld refinement.

Space group = R-3c	$R_{wp} = 4.21\%$	$R_p = 2.95\%$		
$a (\text{\AA}) = 8.96634$	$c (\text{\AA}) = 21.45855$	$\alpha (\text{^\circ}) = 90$		
$\beta (\text{^\circ}) = 90$	$\gamma (\text{^\circ}) = 120$	$V (\text{\AA}^3) = 1494.037$		
Atom	x	y	z	frac
Na1	0.00000	0.00000	0.00000	1.040
Na2	0.64540	0.00000	0.25000	0.971
Mn	0.00000	0.00000	0.15167	0.500
V	0.00000	0.00000	0.14796	0.500
P	0.29869	0.00000	0.25000	1.000
O1	0.02308	0.22138	0.19468	1.000
O2	0.18433	0.16951	0.08177	1.000

Table S3. Surface parameters of the NMVP@C and NMVP@C@CNTs nanocomposite samples.

Sample	BET surface area (m ² g ⁻¹)	BJH pore volume (cm ³ g ⁻¹)	Pore size (nm)
NMVP@C	82.6036	0.174051	8.42827
NMVP@C@CNT	122.4544	0.254544	8.31472
S			

Table S4. ICP-OES analysis of the NMVP@C sample.

Sample	Atomic Ratio / %			
	Na	Mn	V	P
NMVP@C	4.04	1.00	0.99	2.93

Table S5. Comparison of cycling stability of the NMVP@C@CNTs with other $\text{Na}_4\text{MnV(PO}_4)_3$ materials proposed in literature.

Materials	Voltage range (V vs. Na^+/Na)	Cycling stability	Ref.
$\text{Na}_4\text{MnV(PO}_4)_3@\text{C@CNTs}$	2.5-3.8	50 mA h g ⁻¹ after 4000 cycles at 40 C, capacity retention: 68.3%	This work
$\text{Na}_4\text{MnV(PO}_4)_3@\text{C}$	2.5-3.8	~97 mA h g ⁻¹ after 450 cycles at 1 C, capacity retention: ~96%	[3]
$\text{Na}_4\text{MnV(PO}_4)_3@\text{C@GA}$	2.5-3.8	53.7 mA h g ⁻¹ after 4000 cycles at 20 C, capacity retention: 68.8%	[4]
$\text{Na}_4\text{MnV(PO}_4)_3/1\%\text{MWCNTs}$	1.5-4.5	~134 mA h g ⁻¹ after 40 cycles at 0.05 C, capacity retention: ~99.1%	[5]
$\text{Na}_4\text{MnV(PO}_4)_3@\text{C}$	2.5-4.0	~60 mA h g ⁻¹ after 10 cycles at 0.2 C, capacity retention: ~64.5%	[6]
$\text{Na}_4\text{MnV(PO}_4)_3\text{-rGO}$	2.5-3.8	86 mA h g ⁻¹ after 60 cycles at 0.1 C, capacity retention: 91.5%	[7]

■ REFERENCES

- (1) Rui, X. H.; Ding, N.; Liu, J.; Li, C.; Chen, C. H. Analysis of the Chemical Diffusion Coefficient of Lithium Ions in $\text{Li}_3\text{V}_2(\text{PO}_4)_3$ Cathode Material. *Electrochim. Acta* **2010**, *55*, 2384-2390.
- (2) Wang, J.; Polleux, J.; Lim, J.; Dunn, B. Pseudocapacitive Contributions to Electrochemical Energy Storage in TiO_2 (Anatase) Nanoparticles. *J. Phys. Chem. C* **2007**, *111*, 14925-14931.
- (3) Zhou, W.; Xue, L.; Lü, X.; Gao, H.; Li, Y.; Xin, S.; Fu, G.; Cui, Z.; Zhu, Y.; Goodenough, J. B. $\text{Na}_x\text{MV}(\text{PO}_4)_3$ ($\text{M} = \text{Mn, Fe, Ni}$) Structure and Properties for Sodium Extraction. *Nano Lett.* **2016**, *16*, 7836-7841.
- (4) Li, H.; Jin, T.; Chen, X.; Lai, Y.; Zhang, Z.; Bao, W.; Jiao, L. Rational Architecture Design Enables Superior Na Storage in Greener NASICON- $\text{Na}_4\text{MnV}(\text{PO}_4)_3$ Cathode. *Adv. Energy Mater.* **2018**, *8*, 1801418.
- (5) Nisar, U.; Shakoor, R. A.; Essehli, R.; Amin, R.; Orayech, B.; Ahmad, Z.; Kumar, P. R.; Kahraman, R.; Al-Qaradawi, S.; Soliman, A. Sodium Intercalation/De-Intercalation Mechanism in $\text{Na}_4\text{MnV}(\text{PO}_4)_3$ Cathode Materials. *Electrochim. Acta* **2018**, *292*, 98-106.
- (6) Zakharkin, M. V.; Drozhzhin, O. A.; Tereshchenko, I. V.; Chernyshov, D.; Abakumov, A. M.; Antipov, E. V.; Stevenson, K. J. Enhancing Na^+ Extraction Limit through High Voltage Activation of the NASICON-Type $\text{Na}_4\text{MnV}(\text{PO}_4)_3$ Cathode. *ACS Appl. Energy Mater.* **2018**, *1*, 5842-5846.
- (7) Ramesh Kumar, P.; Kheireddine, A.; Nisar, U.; Shakoor, R. A.; Essehli, R.; Amin,

R.; Belharouak, I. Na₄MnV(PO₄)₃-rGO as Advanced Cathode for Aqueous and Non-Aqueous Sodium Ion Batteries. *J. Power Sources* **2019**, *429*, 149-155.